The human TREX-2 complex is stably associated with the nuclear pore basket

David Umlauf[1], Jacques Bonnet[1], François Waharte[2], Marjorie Fournier[1], Matthieu Stierle[1], Benoit Fischer[3], Laurent Brino[3], Didier Devys[1,*] and László Tora[1,*]

[1]Cellular Signaling and Nuclear Dynamics Program, Institut de Génétique et de Biologie Moléculaire et Cellulaire (IGBMC), CNRS UMR 7104, INSERM U964, Université de Strasbourg, BP 10142 – 67404 ILLKIRCH Cedex, CU de Strasbourg, France
[2]Imagerie Cellulaire et Tissulaire, UMR 144, Institut Curie, CNRS, 26 Rue d'Ulm, 75248 Paris Cedex 05, France
[3]High Throughput Screening Facility, Institut de Génétique et de Biologie Moléculaire et Cellulaire (IGBMC), CNRS UMR 7104, INSERM U964, Université de Strasbourg, BP 10142 – 67404 ILLKIRCH Cedex, CU de Strasbourg, France
*Authors for correspondence (devys@igbmc.fr; laszlo@igbmc.fr)

Accepted 19 March 2013
Journal of Cell Science 126, 2656–2667

doi: 10.1242/jcs.118000

Summary

In eukaryotes, mRNA export involves many evolutionarily conserved factors that carry the nascent transcript to the nuclear pore complex (NPC). The THO/TREX complex couples transcription to mRNA export and recruits the mRNA export receptor NXF1 for the transport of messenger ribonucleoprotein particles (mRNP) to the NPC. The transcription and export complex 2 (TREX-2) was suggested to interact with NXF1 and to shuttle between transcription sites and the NPC. Here, we characterize the dynamics of human TREX-2 and show that it stably associates with the NPC basket. Moreover, the association of TREX-2 with the NPC requires the basket nucleoporins NUP153 and TPR, but is independent of transcription. Differential profiles of mRNA nuclear accumulation reveal that TREX-2 functions similarly to basket nucleoporins, but differently from NXF1. Thus, our results show that TREX-2 is an NPC-associated complex in mammalian cells and suggest that it is involved in putative NPC basket-related functions.

Key words: THO/TREX, NXF1, TREX-2, AMEX, Transcription, mRNA export, Nuclear pore complex

Introduction

In eukaryotes, during RNA polymerase II (Pol II) transcription the nascent pre-mRNA transcript undergoes successive and coordinated modifications that include addition of a 5′ 7-methylguanosine cap, splicing, cleavage and polyadenylation of the 3′ end. The complexes involved in the maturation of the pre-mRNA are in general evolutionary well conserved, often interact physically with each other and are recruited co-transcriptionally (for a review, see Moore and Proudfoot, 2009). The nascent mRNA is processed into a transport competent messenger ribonucleoprotein particle (mRNP) that will be addressed to the nuclear pore complex (NPC) for further transport in the cytoplasm and translation by the ribosome. The evolutionarily conserved THO/TREX complex has been shown to couple transcription and mRNA export both in yeast and metazoans (Strässer and Hurt, 2000; Jimeno et al., 2002; Zenklusen et al., 2002; Masuda et al., 2005). Most yeast genes are intronless whereas in metazoans genes usually contain several introns. This difference is reflected in the fact that in yeast, THO/TREX is co-transcriptionally recruited to the mRNP while in metazoans it associates with the splicing machinery (Strässer and Hurt, 2000; Jimeno et al., 2002; Masuda et al., 2005). In metazoans, the THO/TREX complex is formed by the association of the THO complex with two proteins ALY and UAP56 (Yra1 and Sub2 in yeast) which are responsible for the recruitment of the mRNA export receptor NXF1 (Mex67 in yeast) (Piruat and Aguilera, 1998; Strässer and Hurt, 2000; Stutz et al., 2000; Jimeno et al., 2002; Huertas and Aguilera, 2003; Abruzzi et al., 2004; Masuda et al., 2005). NXF1 and Mex67 have been shown to be late actors in the mRNA export pathway and were suggested to transport mRNP particles to the NPC (Segref et al., 1997; Grüter et al., 1998).

The transcription and export complex 2 (TREX-2) is another complex that was initially characterized in yeast and was shown to play a role in mRNA export and gene gating. The yeast TREX-2 complex is composed of five subunits called Sac3, Thp1, Cdc31, Sus1 and Sem1 and it interacts with the inner face of the NPC via the basket nucleoporin Nup1, the human NUP153 ortholog. In yeast, deletion of any TREX-2 subunits results in mRNA export defects (Fischer et al., 2002; Fischer et al., 2004; Rodríguez-Navarro et al., 2004; Wilmes et al., 2008; Faza et al., 2009). Orthologous complexes have been isolated in *Drosophila* (where the complex is called AMEX for Anchoring and mRNA Export) and plants (Kurshakova et al., 2007; Lu et al., 2010). Although its exact composition remains to be determined, AMEX is predominantly localized at the nuclear side of the NPC and appears to recapitulate the functions described in yeast.

More recently, *in vitro* pull-down assays demonstrated that two independent regions of human GANP (Sac3 homologue) interact with ENY2 and CETN2/CETN3 (Sus1 and Cdc31 homologues) on one hand and with PCID2 and DSS1 (Thp1 and Sem1 homologues) on the other hand (Jani et al., 2012). Structural analysis of recombinant GANP-ENY2 complex revealed that GANP binds two ENY2 molecules similarly to yeast where Sac3 was shown to be the scaffold protein onto which all other subunits assemble (Jani et al., 2009; Ellisdon et al., 2012; Jani et al., 2012). In human, depletion of most TREX-2 subunits

results in mRNA nuclear accumulation. Some subunits such as GANP, ENY2 and CETN2 were shown to associate with the nuclear envelope where GANP is required for ENY2 localization (Wickramasinghe et al., 2010; Jani et al., 2012). Conversely, ENY2 depletion did not affect GANP localization. Based on interactions detected between GANP, the RNA polymerase II largest subunit, NXF1 and NUP153, it has been proposed that TREX-2 is required for the shuttling of competent mRNP particles from transcription sites to the NPC.

Interestingly, the TREX-2 subunit Sus1 is shared with the transcriptional coactivator complex Spt-Ada-Gcn5 acetyltransferase (SAGA) and it was suggested that gene gating of specific yeast genes depends on the ability of SAGA to recruit TREX-2 for proper targeting (Rodríguez-Navarro et al., 2004; Cabal et al., 2006; Köhler et al., 2008). In human and yeast ENY2/Sus1 interacts with the ATXN7L3/Sgf11 protein of SAGA and together regulate its histone deubiquitination activity (Köhler et al., 2006; Zhao et al., 2008; Köhler et al., 2010; Samara et al., 2010). Strikingly, the ENY2/Sus1 fold wraps around a long α-helix found in both GANP/Sac3 and the SAGA subunit ATXN7L3/Sgf11 (Ellisdon et al., 2010) suggesting that ENY2/Sus1 could play an important structural and/or regulatory role in both complexes.

We show here that the association of the TREX-2 complex with the NPC is extremely stable in human cells. Unexpectedly, our live cell imaging experiments show that the dynamics of TREX-2 at the nuclear periphery is comparable to the one described for scaffold nucleoporins. Interestingly, mRNA export defects after TREX-2 subunits (GANP and ENY2) or pore basket component (NUP153 and TPR) depletion were highly similar but strikingly milder than that observed after the mRNA export receptor NXF1 knockdown. Therefore, TREX-2 is an NPC-basket-associated complex whose localization appears to be independent of ongoing transcription.

Results

TREX-2 is localized at the nuclear periphery independently of the SAGA complex

To determine whether the human TREX-2 and SAGA interact with each other and are functionally linked like their homologous yeast complexes, we generated two HeLa cell lines stably expressing either ENY2 or the SAGA specific SPT3 subunit tagged with a FLAG-HA peptide. ENY2-FLAG-HA and FLAG-HA-SPT3 proteins were purified from nuclear extracts by successive FLAG and HA immunoprecipitations (Nakatani and Ogryzko, 2003) and the associated proteins were analyzed either by gel-based nanoflow LC-MS/MS or non-gel-based Multi Dimensional Protein Identification Technology (MudPIT) mass spectrometry methods. As expected, peptides corresponding to all known SAGA subunits were identified in both purifications. In contrast, the ENY2-FLAG-HA but not the FLAG-HA-SPT3 immunoprecipitation recovered all putative TREX-2 subunits (supplementary material Fig. S1A). Our Mass Spectrometry analyses suggest that TREX-2 would be composed of GANP, PCID2, ENY2 and either CETN2 or CETN3. Note that DSS1 was not detected as this small protein may produce few peptides after trypsin digestion (supplementary material Fig. S1B). The association of ENY2 with both SAGA and TREX-2 was further confirmed by western-blot analysis using our newly developed rabbit polyclonal antibodies against GANP and PCID2 as well as CETN3 (Giessl et al., 2004) and SAGA specific antibodies (Mengus et al., 1995; Brand et al., 2001; Helmlinger et al., 2004; Zhao et al., 2008; Nagy et al., 2009) (Fig. 1A). In our FLAG-HA-SPT3 purifications we identified only SAGA subunits, but no subunits of the TREX-2 complex suggesting that SAGA and TREX-2 do not interact under our experimental conditions. To rule out the possibility that the interactions between the TREX-2 subunits are RNA mediated we performed the same experiment at physiological salt concentrations with or without addition of RNase A in the nuclear extracts and during the immunoprecipitation. This experiment indicated that RNA is not involved in the formation of the TREX-2 complex (Fig. 1B; supplementary material Fig. S1). The normalized spectral abundance factor (Paoletti et al., 2006) for TREX-2 and SAGA subunits as determined from the MudPIT analyses indicated that in HeLa cell nuclei TREX-2 is more abundant than SAGA. Together, these data confirm that ENY2 is part of both human SAGA and TREX-2 complexes and do not support an interaction between the two complexes (Fig. 1A,B; supplementary material Fig. S1).

Next we used the ENY2-FLAG-HA and FLAG-HA-SPT3 cells to determine the cellular localization of the TREX-2 complex by performing indirect confocal immunofluorescence (IF) experiments. The tagged-ENY2 displayed a strong and punctuated signal at the nuclear periphery as well as a weak diffuse nuclear staining (Fig. 1C). In contrast, FLAG-HA-SPT3 showed a faint and diffuse nuclear staining whereas no FLAG staining was detectable in the parental HeLa cells. These results, in agreement with the above biochemical data, further suggest that ENY2 is present in two different complexes having different cellular localizations. In addition, our IF experiments in parental HeLa cells using antibodies specific for different TREX-2 subunits showed that GANP is localized predominantly at the nuclear envelope while PCID2 is found at the nuclear periphery along with a cytoplasmic and nuclear staining. Finally, both CETN2 and CETN3 localized at the centriole as reported earlier (Middendorp et al., 1997; Trojan et al., 2008; Resendes et al., 2008) and also displayed a perinuclear staining (Fig. 1D; supplementary material Fig. S2). Similar results were obtained by using the same antibodies in ENY2-FLAG-HA and FLAG-HA-SPT3 expressing cells (supplementary material Fig. S2A,B). These observations further suggest that TREX-2 and SAGA have different cellular localizations and do not support a functional coupling of these two complexes.

TREX-2 is located at the NPC

To determine where the TREX-2 complex is localized at the nuclear envelope, we generated HeLa cells stably expressing either ENY2 or PCID2 fused to the EGFP protein. Independent EGFP-ENY2 and EGFP-PCID2 clones expressing the recombinant proteins at lower levels than the corresponding endogenous ones were selected and showed a distribution of the fluorescent protein that recapitulated the signal obtained by IF for ENY2-FLAG-HA and PCID2 (Fig. 2A; supplementary material Fig. S3). Moreover, both fusion proteins kept their perinuclear localization upon depletion of the corresponding endogenous proteins after treatment with small interfering RNA (siRNA) targeting the 3′UTR of the corresponding mRNA (see below). Biochemical evidence showed that EGFP-ENY2 is integrated in the endogenous TREX-2 complex (supplementary material Fig. S3D).

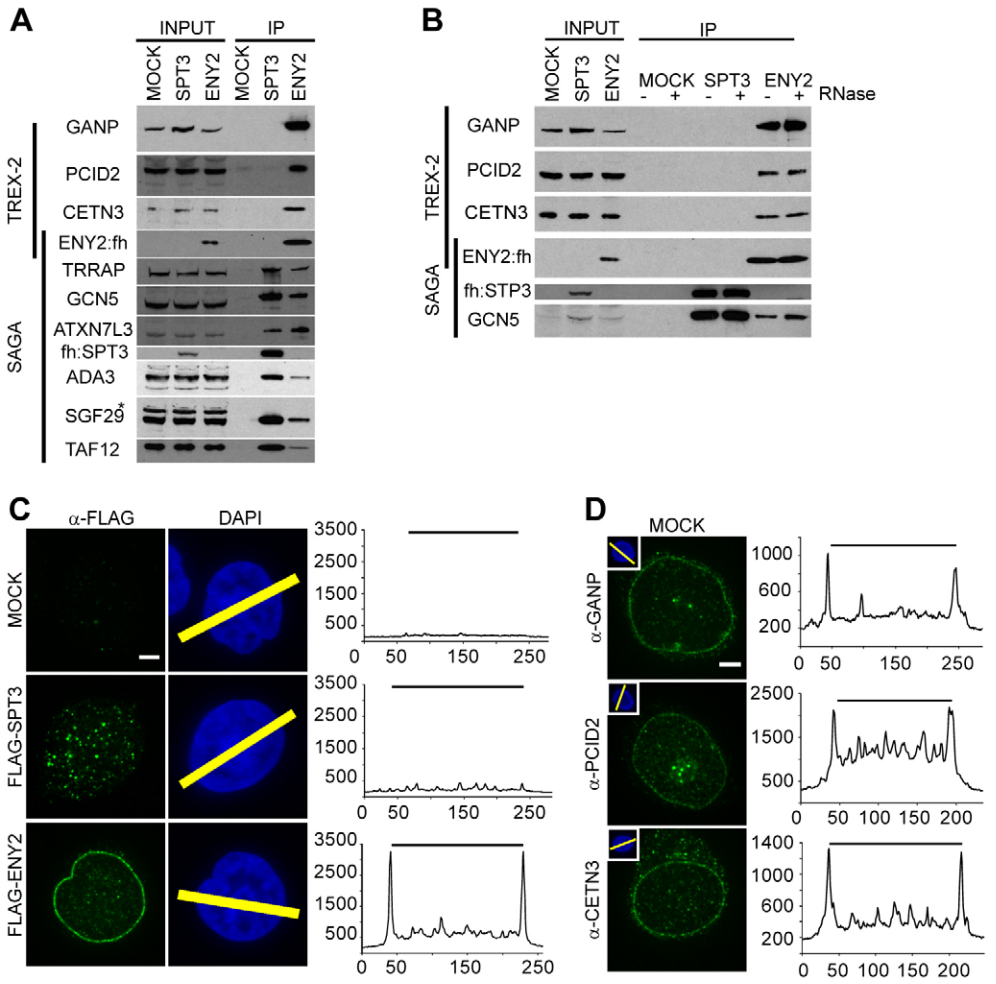

Fig. 1. ENY2 is a subunit of the TREX-2 complex that localizes at the nuclear periphery independent of SAGA. (**A**) Western blot of mock, FLAG-HA-SPT3 and ENY2-FLAG-HA immunoprecipitations probed with anti-TREX-2 and anti-SAGA antibodies as indicated. Asterisks indicate non-specific bands; fh, FLAG-HA. (**B**) Western blot analysis of immunoprecipitations performed as in A, with or without addition of RNase A, using anti-TREX-2 and anti-SAGA antibodies as indicated. (**C**) Parental, FLAG-HA-SPT3 and ENY2-FLAG-HA HeLa cells were stained with α-FLAG antibody and analyzed by confocal microscopy. Charts indicate the fluorescence distribution in the yellow region highlighted in the DAPI staining of the corresponding cell. The black bar represents the nuclear interior. (**D**) HeLa cells were stained with α-GANP (2988), α-PCID2 (2990) and α-CETN3 antibodies. Charts indicate the fluorescence distribution in the yellow region highlighted in the DAPI staining shown as an inset in the corresponding stained cell. The black bar represents the nuclear interior. Scale bars: 5 μm.

To study the distribution of EGFP-ENY2 and EGFP-PCID2 relative to the other subunits of the complex or the NPC we performed IF using anti-TREX-2 or anti-NPC specific antibodies using confocal microscopy. In all cases the extent of colocalization between EGFP-ENY2 or EGFP-PCID2 and the other TREX-2 subunits at the nuclear periphery was significant suggesting that the TREX-2 complex can also be detected in intact cells. Moreover, the colocalization signal between ENY2 and the NPC was almost complete showing that TREX-2 colocalizes with NPCs at the nuclear periphery (Fig. 2A).

In agreement with a former study showing that GANP interacts with the mRNA export receptor NXF1 (Wickramasinghe et al., 2010), we could show that NXF1 colocalizes with EGFP-ENY2 and EGFP-PCID2 at the nuclear periphery (Fig. 2A; supplementary material Fig. S3B). However, NXF1 did not colocalize with the tested TREX-2 subunits in the nucleoplasm. In control cells stably expressing EGFP alone, no such colocalization was detectable between GANP and EGFP. Altogether these results suggest that all subunits of the complex localize at the NPC.

To further determine on which side of the nuclear envelope the TREX-2 complex localizes, cells were treated with 0.004% digitonin to permeabilize the cytoplasmic but not the nuclear membranes. Under these conditions, proteins localized at the outer but not the inner face of the nuclear envelope can be labeled by immunofluorescence. As a control, cells were permeabilized with Triton X-100 which allows the detection of proteins associated with both sides of the nuclear membrane. As previously described, RANBP2 was found on the cytoplasmic side whereas Lamin A/C was exclusively revealed on the nuclear side (Fig. 2B). Our experiments show that all TREX-2 subunits are exclusively localized at the inner face of the nuclear membrane (Fig. 2C; supplementary material Fig. S4).

TREX-2 localization at the NPC depends on the basket nucleoporins NUP153 and TPR

To better characterize TREX-2 function at the NPC we used siRNA to deplete cells for NUP153 and TPR, two nucleoporins that belong to the nuclear pore basket (Sukegawa and Blobel, 1993; Frosst et al., 2002) and assessed TREX-2 localization by IF. Cells knocked-down for NUP153 or TPR show a complete disappearance of GANP and CETN3 from the nuclear periphery (Fig. 3A). Similarly, there was a strong reduction of the perinuclear staining of EGFP-ENY2 in the corresponding cell line (Fig. 3B). These results indicate that NUP153 and TPR are required for TREX-2 interaction with the NPC and more specifically the nuclear basket.

We next investigated whether removing TREX-2 from the NPC basket would in turn have an influence on the localization of TPR. To this aim we depleted cells for GANP the scaffold protein of the TREX-2 complex. Although GANP depletion results in the disappearance of the perinuclear CETN3 and EGFP-ENY2 signal

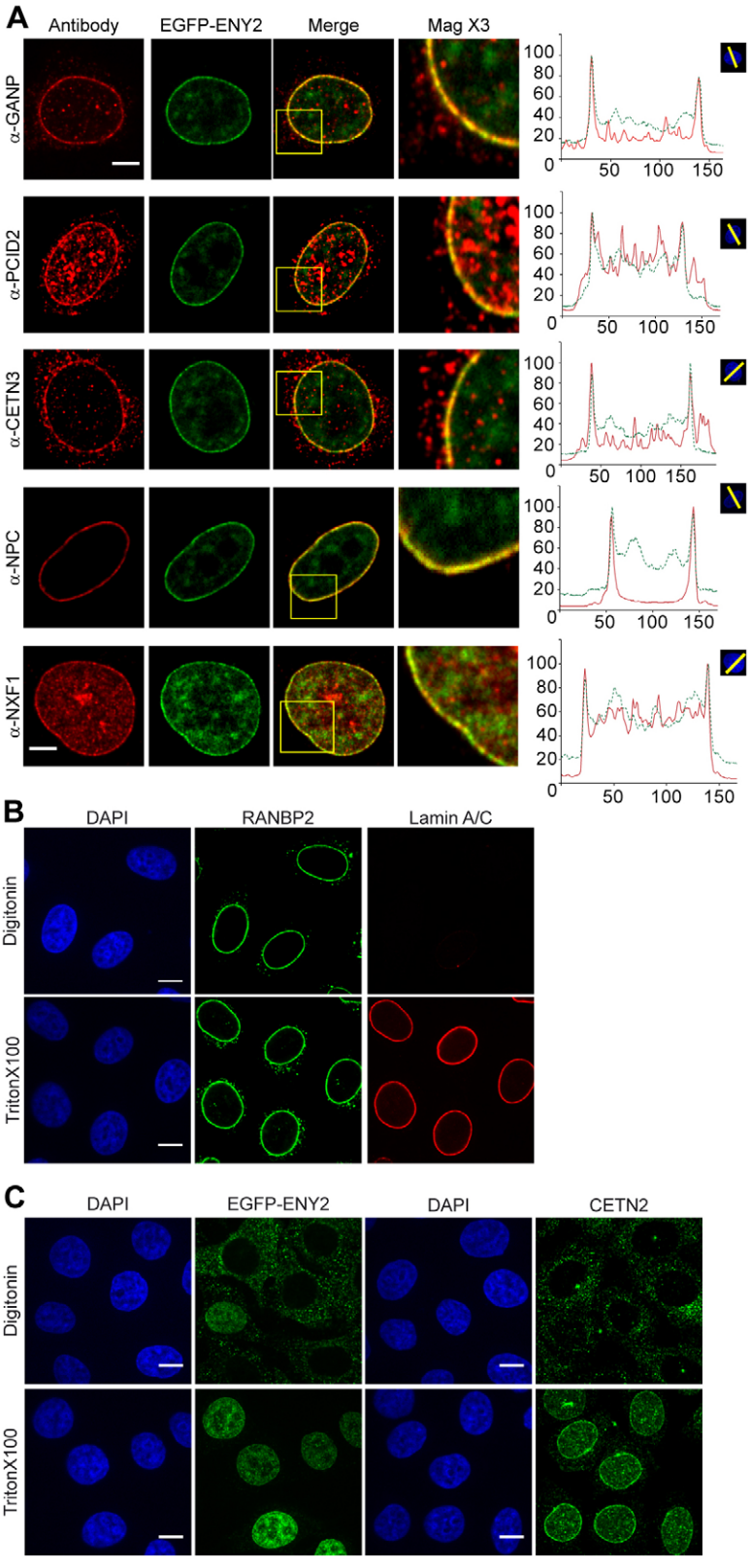

Fig. 2. All TREX-2 subunits colocalize with the NPC. (**A**) HeLa cells stably expressing EGFP-ENY2 were stained with α-GANP (2988), α-PCID2 (2990), α-CETN3, α-NPC and α-NXF1 antibodies. An inset of the merge signals is shown and represents a 3× magnification of the selected region (yellow square). Charts on the right depict the distribution of the fluorescence (in green for EGFP-ENY2 and red for the corresponding antibody) as measured across the yellow region highlighted on the DAPI staining (top right corner of each chart). The *x*-axis represents the distance in pixels; the *y*-axis represents the intensity distribution in arbitrary units.(**B**,**C**) Hela cells were fixed and permeabilized with 0.004% digitonin or 0.1% Triton X-100 and stained with α-RANBP2, α-Lamin A/C, α-EGFP or α-CETN2 antibodies as indicated. Scale bars: 5 μm.

in the corresponding cell line, it does not influence the localization of TPR suggesting that TREX-2 is not reciprocally important for TPR localization (Fig. 3). It is noteworthy that depletion of NUP153, TPR or GANP do not influence the cellular localization of the mRNA export receptor NXF1 (Fig. 3). This would suggest that TREX-2 and nuclear basket nucleoporins are dispensable for the recruitment of NXF1-associated mRNPs at the NPC.

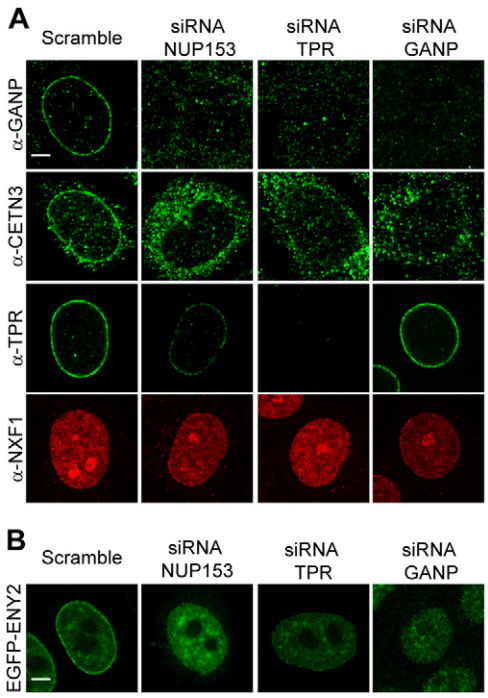

Fig. 3. TREX-2 localization at the NPC depends on the basket nucleoporins NUP153 and TPR. (**A**,**B**) HeLa cells (A) or EGFP-ENY2 stably-expressing cells (B) were transfected with scramble siRNA or siRNAs targeting NUP153, TPR or GANP for 72 hours. Cells were then stained with α-GANP (2988), α-CETN3 and α-TPR antibodies and analyzed by confocal microscopy. Cells stained with the α-TPR antibody were co-stained with a α-NXF1antibody. Scale bars: 5 μm.

GANP and ENY2 are crucial for TREX-2 interaction with the nuclear pore basket

Next, to identify the TREX-2 subunits important for the *in vivo* stability of the complex and for the interaction with the nuclear basket we undertook a systematic knockdown approach using specific siRNAs against the different subunits. Cells transfected with scramble siRNA showed the expected perinuclear staining for GANP, PCID2, CETN3, EGFP-ENY2 and EGFP-PCID2. GANP-depleted cells showed a complete disappearance of PCID2 and CETN3 staining from the nuclear basket suggesting that either GANP is required for TREX-2 assembly or that it anchors the complex at the NPC (Fig. 4A). These results are in good agreement with available structural data (Jani et al., 2009; Ellisdon et al., 2012; Jani et al., 2012) indicating that GANP is the scaffold protein of the TREX-2 complex. In EGFP-ENY2 cells depletion of GANP induced a complete loss of the perinuclear fluorescence along with a strong reduction of the diffuse nuclear signal. Similar loss of fluorescence from the nuclear periphery occurred in EGFP-PCID2 cells following GANP knockdown (Fig. 4B).

Strikingly, siRNA depletion of ENY2 led to a significant loss of GANP, PCID2 and CETN3 signals from the nuclear envelope as compared to the control scramble siRNA treatment. Consistent with this, EGFP-PCID2 cells also lost their perinuclear fluorescence after ENY2 depletion (Fig. 4A,B). To determine the influence of the two other subunits on TREX-2 localization, cells were transfected with siRNA against PCID2 and CETN3. Despite reduction of both PCID2 and CENT3 protein and mRNAs, we did not observe changes in the staining of the GANP and ENY2 subunits (supplementary material Fig. S5). These data together indicate that GANP and ENY2 are crucial for anchoring TREX-2 to the NPC basket as opposed to PCID2 and CETN3 that are dispensable and do not influence its stability.

GANP and ENY2 influence each other's stability

Since we observed a decrease of the EGFP-ENY2 fluorescence upon GANP knockdown, we further investigated TREX-2 stability. Western-blot analysis of GANP depleted cells revealed a strong reduction of GANP that was accompanied by a similar reduction in EGFP-ENY2. However, total cellular PCID2 and CETN3 protein levels were unchanged. In addition, upon ENY2 depletion GANP protein level was reproducibly diminished whereas PCID2 and CETN3 levels were unaffected (Fig. 4C,D; supplementary material Fig. S5).

Since ENY2 also belongs to the deubiquitination module of SAGA (Köhler et al., 2010; Samara et al., 2010; Lang et al., 2011) we tested whether its depletion would affect the stability of its interaction partner ATXN7L3. Indeed, ATXN7L3 was almost undetectable in the cells treated with siRNA targeting ENY2, suggesting that ENY2 is crucial for the stability of its two interaction partners GANP and ATXN7L3 (Fig. 4D). The ENY2-dependent stability of GANP and ATXNL3 is likely regulated by the proteasome pathway. In fact ATXNL3 levels were partially recovered upon treatment of ENY2 depleted cells with the proteasome inhibitor MG132 (Fig. 4E). Thus, GANP and ENY2 are reciprocally important for each other's stability hence explaining the destabilization of TREX-2 and its disappearance from the NPC upon GANP or ENY2 knockdown.

TREX-2 association with the nuclear pore basket is highly stable

As TREX-2 localizes at the NPC basket we sought to determine the dynamics of EGFP-ENY2 and EGFP-PCID2 in relation to other known mRNA export factors. We first assessed the dynamics of NXF1 using cells transiently expressing EYFP-NXF1 and performed fluorescence recovery after photobleaching (FRAP) experiments. In transfected cells, EYFP-NXF1 localized both at the nuclear periphery and in the nuclear interior similarly to the staining obtained by immunofluorescence on the endogenous protein (Fig. 2). After photobleaching a perinuclear region we observed a complete recovery of fluorescence in 12 seconds (Fig. 5A). This fast exchange of NXF1 at the nuclear periphery is in good agreement with the described role of NXF1 in transporting mRNP particles to NPCs (Segref et al., 1997). Surprisingly, similar FRAP experiments performed with EGFP-ENY2 and EGFP-PCID2 stable cells showed a fluorescence recovery of about seven hours for EGFP-ENY2 and eighty minutes for EGFP-PCID2 (Fig. 5A). These results indicate that in contrast to NXF1, the turnover of EGFP-ENY2 and EGFP-PCID2 at the nuclear periphery is very slow. Therefore, TREX-2 seems to be stably associated with the nuclear pore basket as its dynamics is in range with the one previously described for the nucleoporins of the NPC core structure (Rabut et al., 2004).

As the basket nucleoporin NUP153 is necessary for TREX-2 association with the NPC (Fig. 3), we analyzed the dynamics of this protein using cells transiently transfected with a construct expressing EGFP-NUP153. These cells displayed a typical NPC like signal and after perinuclear photobleaching we observed complete fluorescence recovery in 10 minutes (Fig. 5A). The

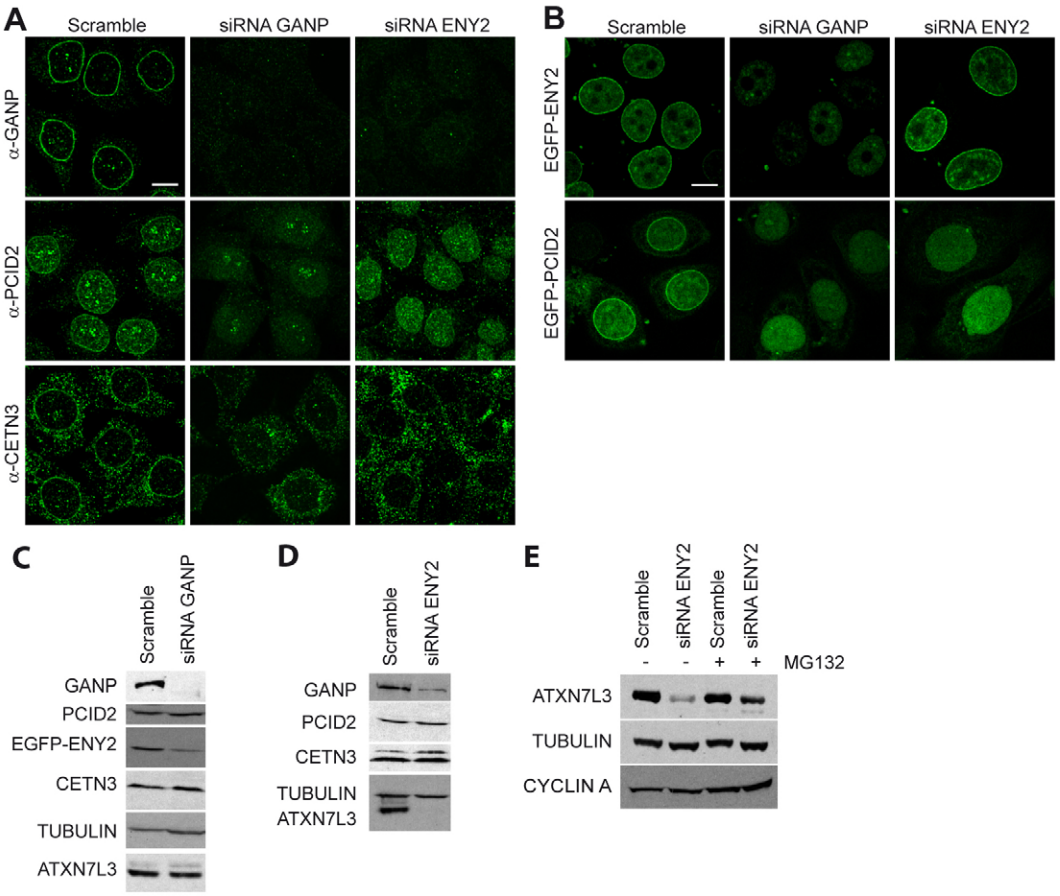

Fig. 4. GANP and ENY2 are crucial for TREX-2 stability and localization at the nuclear pore basket. (**A**,**B**) HeLa cells (A) or EGFP-ENY2 and EGFP-PCID2 (B) stable cells were transfected with scramble siRNA or siRNAs targeting GANP or ENY2 for 72 hours. (A) HeLa cells were then stained with α-GANP (2988), α-PCID2 (2990) and α-CETN3 antibodies and analyzed by confocal microscopy. (B) The EGFP-ENY2 or EGFP-PCID2 fluorescence was analyzed by confocal microscopy. The ENY2-specific siRNA used in this experiment targets the 5′UTR of the corresponding gene and therefore did not affect EGFP-ENY2. (**C**,**D**) Cells were transfected with scramble siRNA or siRNAs targeting GANP (C) or ENY2 (D). Whole cell extracts were prepared 72 hours after transfection and western blot analyses were carried out and probed as indicated. (**E**) HeLa cells were transfected with scramble or ENY2-specific siRNAs. After 48 hours, half the samples were subjected to proteasome inhibition using MG132 for another 15 hours and whole cell extracts prepared. Western blot analyses were carried out and probed as indicated. Scale bars: 5 μm.

NUP153 recovery results are similar to the one obtained in rat NRK cells (Rabut et al., 2004) and demonstrate that TREX-2 association with the NPC is even more stable than that of NUP153 suggesting that other nucleoporins may be required for TREX-2 tethering to the NPC.

To further confirm our observations and to assess the exchange of EGFP-ENY2 and EGFP-PCID2 proteins between the nucleoplasm and the NPC associated fractions, we performed fluorescence loss in photobleaching (FLIP) experiments. Repetitive photobleaching of a selected area of the nucleus resulted in a complete loss of the EGFP-ENY2 or EGFP-PCID2 fluorescence in the nucleoplasm in less than 10 minutes revealing the existence of a dynamic pool of both proteins in this compartment. Strikingly, this fast moving pool did not exchange with the NPC associated fraction that remained unaffected during the analysis (Fig. 5B). On the contrary, photobleaching the nuclear pool of EYFP-NXF1 resulted in the disappearance of the perinuclear staining indicating that NXF1 can move not only within the nucleoplasm but also from the nuclear periphery to the interior (Fig. 5B). Thus, our results together demonstrate that TREX-2 association with the NPC basket is extremely stable in contrast to NXF1 that can exchange between the nucleoplasm and the nuclear periphery consistent with its role as an mRNA export receptor.

In higher eukaryotes mitosis is characterized by the disassembly of the nuclear envelope around pro-metaphase and its reassembly during anaphase and telophase coincides with the reformation of NPCs [see for review (Antonin et al., 2008)]. While nucleoporins such as the NUP107-160 subcomplex re-associate with the nuclear envelope in early anaphase, others like TPR or GP210 relocalize to the NPC only in G1 (Bodoor et al., 1999; Dultz et al., 2008; Burke and Ellenberg, 2002). To determine the timing of EGFP-ENY2 re-association with the NPC basket during mitosis, we performed time lapse imaging experiments. The signal of EGFP-ENY2 decreases soon after cells have entered metaphase while upon completion of cytokinesis it relocalizes to the nucleus with a clear perinuclear signal in G1 (Fig. 5C). Together, these observations demonstrate that TREX-2 reassembles with the NPC in G1 like the basket nucleoporin TPR (Bodoor et al., 1999).

TREX-2 association with the nuclear pore basket is transcription independent

The TREX-2 complex has recently been suggested to interact with the transcription machinery (Jani et al., 2012). To determine if the stable association of TREX-2 with the NPC basket is transcription dependent we tested the effect of the transcription inhibitors Actinomycin D and α-amanitin on the nuclear distribution of TREX-2. Incorporation of 5-fluorouridine (5FU) was used as a marker to assess the efficiency of transcription inhibition (Dimitrova, 2006) and revealed a dramatic reduction in the levels of nascent transcripts (Fig. 6). Transcription inhibition induced a global decrease and redistribution of the active form of Pol II in the nucleus (supplementary material Fig. S6) but did not affect TREX-2 distribution as both EGFP-ENY2 and EGFP-PCID2 remained stable at the NPC (Fig. 6A). To assess the influence of transcription inhibition on endogenous TREX-2 subunits we tested the effect of Actinomycin D on the localization of endogenous GANP and CETN3 in HeLa cells (Fig. 6B). GANP and CETN3 displayed the same perinuclear localization in untreated and Actinomycin D treated cells. Identical results were observed when live cells were permeabilized prior to fixation thus allowing soluble proteins to flow out of the cell. Taken together these data unambiguously demonstrate that TREX-2 is stably associated with the nuclear envelope and that this localization is transcription independent in HeLa cells.

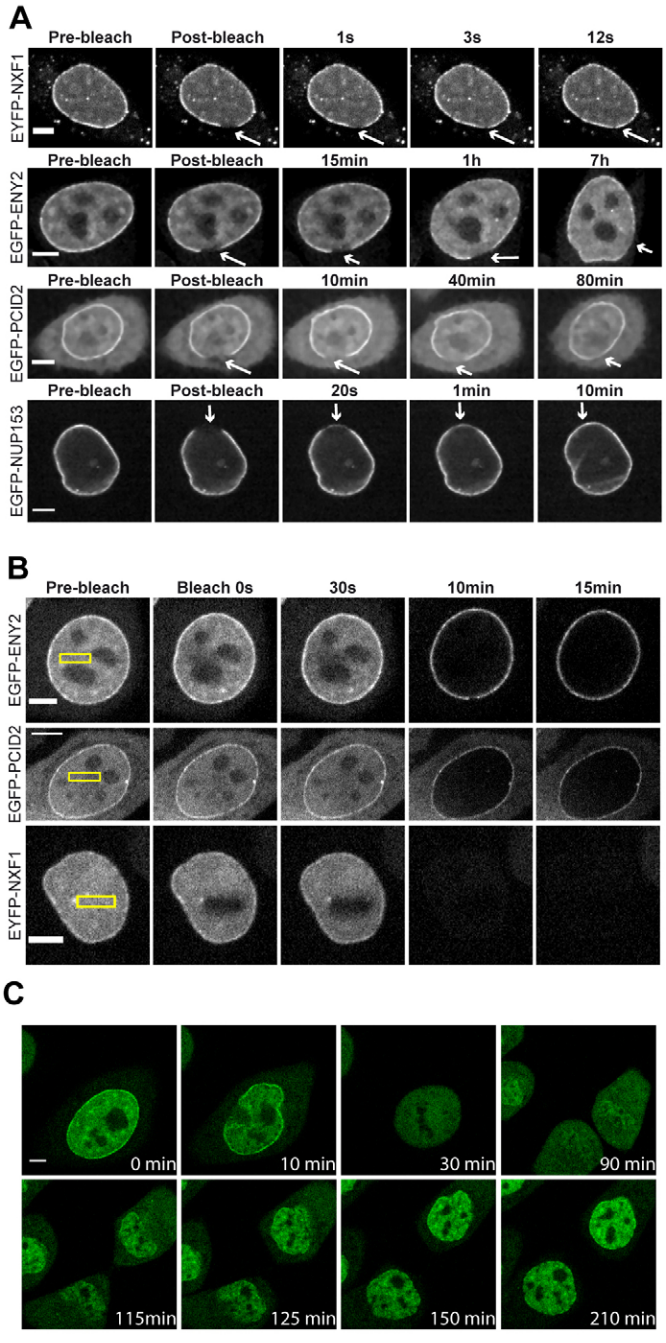

Fig. 5. TREX-2 association with the nuclear pore basket is highly stable *in vivo*. (**A**) FRAP experiments were performed on nine EYFP-NXF1, five EGFP-ENY2, six EGFP-PCID2 and fifteen EGFP-NUP153 expressing cells. Representative images of fluorescence recovery at a photobleached perinuclear region are shown (white arrows). Time after photobleaching is indicated on top of each panel. (**B**) Six EGFP-ENY2, six EGFP-PCID2 and seven EYFP-NXF1 expressing cells were analyzed by FLIP. Representative images show the nuclear fluorescence during repetitive photobleaching of the nucleoplasmic area (rectangles as indicated in the pre-bleach panels) of EGFP-ENY2, EGFP-PCID2 and EYFP-NXF1. Photobleaching was carried out every 30 seconds. After 10–15 minutes, fluorescence of EYFP-NXF1 totally disappears from the nucleus as opposed to a stable EGFP-ENY2 and EGFP-PCID2 perinuclear signal. (**C**) Time-lapse imaging of EGFP-ENY2 cells during mitosis. Cells were imaged for 24 hours with an acquisition every 5 minutes. Images were acquired on the *z*-axis with a step of 1 µm. Selected *z*-stacks for EGFP-ENY2 are shown. These experiments were performed on EGFP-ENY2 and EGFP-PCID2 stable cell lines whereas other constructions were transiently transfected. Scale bars: 5 µm.

TREX-2 subunit knockdown results in similar mRNA export defects as those observed with NUP153 and TPR

TREX-2 has been reported to be involved in the export of poly(A)$^+$ mRNA through its interaction with the mRNA export receptor NXF1. It was proposed that TREX-2 bound to NXF1 is shuttling between the nucleoplasm and the NPC where it interacts with NUP153 (Wickramasinghe et al., 2010; Jani et al., 2012). In contrast to this model our results show that TREX-2 is stably associated with the NPC. Therefore, we investigated whether TREX-2 could facilitate the nucleocytoplasmic transport of mRNP particles directly at the nuclear pore basket. We analyzed the distribution of poly(A)$^+$ mRNA in the nucleus by fluorescence *in situ* hybridization (FISH) following siRNA knockdown of different TREX-2 subunits as well as the basket nucleoporins NUP153 and TPR in both HeLa and HCT116 cells. As a positive control for mRNA export defect, we used siRNA directed against NXF1 and observed a massive accumulation of poly(A)$^+$ mRNA in both cell types consistent with this protein being one of the main mRNA export factor. In contrast, depletion of GANP or ENY2 leads to a milder but reproducible poly(A)$^+$ mRNA nuclear retention. Interestingly the FISH pattern observed after GANP or ENY2 depletion was very similar to that seen in NUP153 or TPR knockdown cells (Fig. 7). In both cell lines, we observed a clear difference between NXF1 and the other tested proteins although mRNA nuclear retention after downregulation of NUP153, TPR, GANP and ENY2 was consistently higher in HCT116 than in HeLa cells. Instead of an homogenous accumulation throughout the nucleus, depletion of NUP153, TPR, GANP or ENY2 in HeLa cells seems to have an effect on

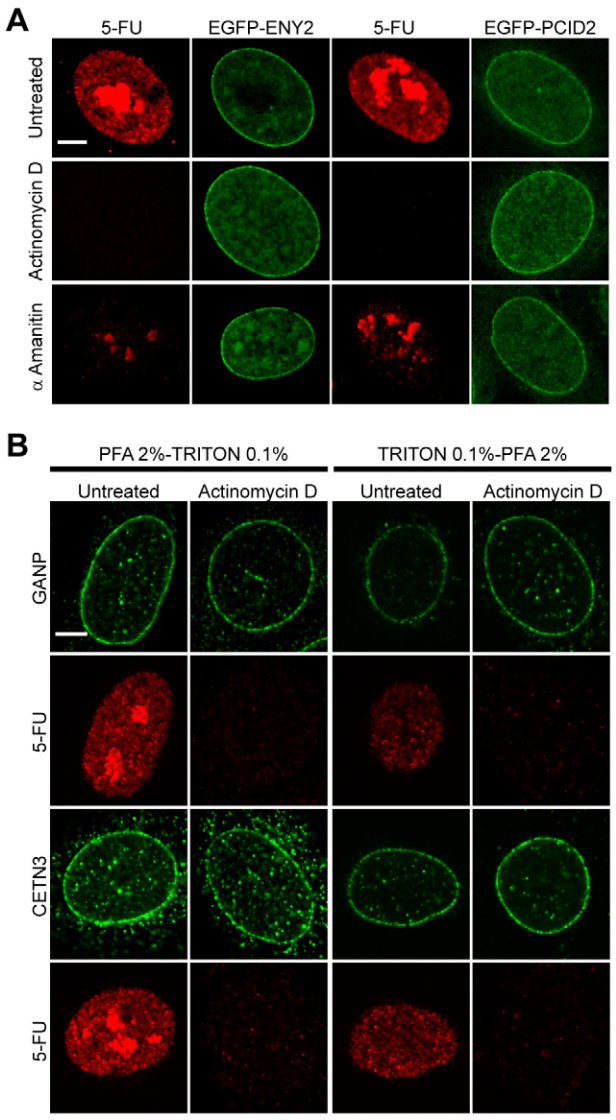

Fig. 6. TREX-2 localization at the nuclear pore basket is independent of transcription by RNA polymerase II. (**A**) EGFP-ENY2 or EGFP-PCID2 stable cells were treated with actinomycin D or α amanitin for 4–6 hours. Transcription inhibition was monitored by incubating the cells with 5-FU for 20 minutes. Incorporation into nascent transcripts was revealed using an α-5-FU antibody. Cells were analyzed using confocal microscopy. (**B**) HeLa cells were treated with actinomycin D for 4–6 hours and incubated with 5-FU for another 20 minutes. Two different protocols were then applied. Cells were either fixed with 2% formaldehyde and then permeabilized using 0.1% Triton X-100 or cells were permeabilized first using 0.1% Triton X-100 for 5 minutes on ice and then fixed using 2% formaldehyde. Cells were then co-stained with an α-5-FU antibody and α-GANP (2988) or α-CETN3 antibodies and analyzed by confocal microscopy. Scale bar: 5 μm.

the number and the size of the nuclear poly(A)$^+$ mRNA foci (supplementary material Fig. S7). Consistent with the above observations, NXF1 depletion led to a high rate of cell death in both cell types (data not shown) which was not observed after knockdown of any TREX-2 component further emphasizing the functional differences between those mRNA export components. As NUP153 and TPR are necessary for TREX-2 localization to the NPC basket but not vice versa (Fig. 3) and as TREX-2 subunit knockdowns mimic the mRNA nuclear retention observed with NUP153 and TPR, it is conceivable that the correct function of NUP153 and TPR in mRNA export is dependent on TREX-2 anchoring at the NPC basket.

Discussion

Here we have characterized the human TREX-2 complex using biochemical and cellular approaches. We show that TREX-2 association with the NPC is extremely stable and independent of ongoing transcription. This association requires the basket nucleoporins NUP153 and TPR whereas in turn TREX-2 seems dispensable for the localization of these proteins at the nuclear basket. Within TREX-2, GANP and ENY2 are crucial for the stability and the localization of the complex at the NPC whereas PCID2 and CETN3 appear dispensable. Furthermore we have shown that GANP and ENY2 influence each other's stability and therefore the localization of TREX-2. This contrasts with a previous report suggesting that ENY2 is not important for GANP localization at the NPC (Jani et al., 2012). In support of our data, we show that ENY2 is crucial to stabilize not only GANP but also ATXN7L3, its interaction partner within SAGA.

Our analyses consistently demonstrate that TREX-2 is tightly bound to the NPC as opposed to NXF1 suggesting that their respective roles in mRNA export can be uncoupled. Our conclusions are supported by several lines of evidence that all point to a unique model for TREX-2 function at the NPC basket: (i) Our FRAP experiments unambiguously uncovered a highly stable association of TREX-2 with the NPC as opposed to the dynamic association of NXF1 with this structure. (ii) In contrast to NXF1, the NPC-associated fraction of ENY2 does not exchange with its nucleoplasmic fraction excluding any shuttling of TREX-2 between these two compartments. (iii) Following mitosis, ENY2 re-associates with the NPC in early G1 similarly to other nucleoporins such as TPR and GP120. (iv) poly(A)$^+$ mRNA nuclear accumulation observed after knockdown of TREX-2 subunits or basket nucleoporins are highly similar and much milder than that seen in NXF1 depleted cells. (v) The perinuclear localization of NXF1 was not altered following depletion of either basket nucleoporins or TREX-2 subunits. (vi) TREX-2 localization at the NPC was found to be independent of ongoing transcription. (vii) Most of the above described results were obtained in two different human cell lines therefore excluding cell type specificity and more likely reflecting the general properties of TREX-2 in mammalian cells (supplementary material Fig. S8).

Previous models suggesting that TREX-2 is shuttling between sites of active transcription and the NPC are not supported by our results (Jani et al., 2012). In agreement with a former study (Wickramasinghe et al., 2010) we showed that GANP localization is not altered in NXF1 depleted cells. However, in striking contrast, depletion of TREX-2 subunits or basket nucleoporins did not affect NXF1 localization. Previous studies have shown that NXF1 is involved in the export of the pre-60S ribosomal particle that is independent of the mRNA export pathway and that its yeast orthologue can interact with the core scaffold NUPs independent of the NPC basket (Yao et al., 2007; Yao et al., 2008). Therefore, a significant fraction of NXF1 is expected to be localized at the NPC even after depletion of the nuclear pore basket. However, we cannot rule out the possibility that a fraction of NXF1-bound mRNP particles binds to TREX-2 at the NPC basket for further export.

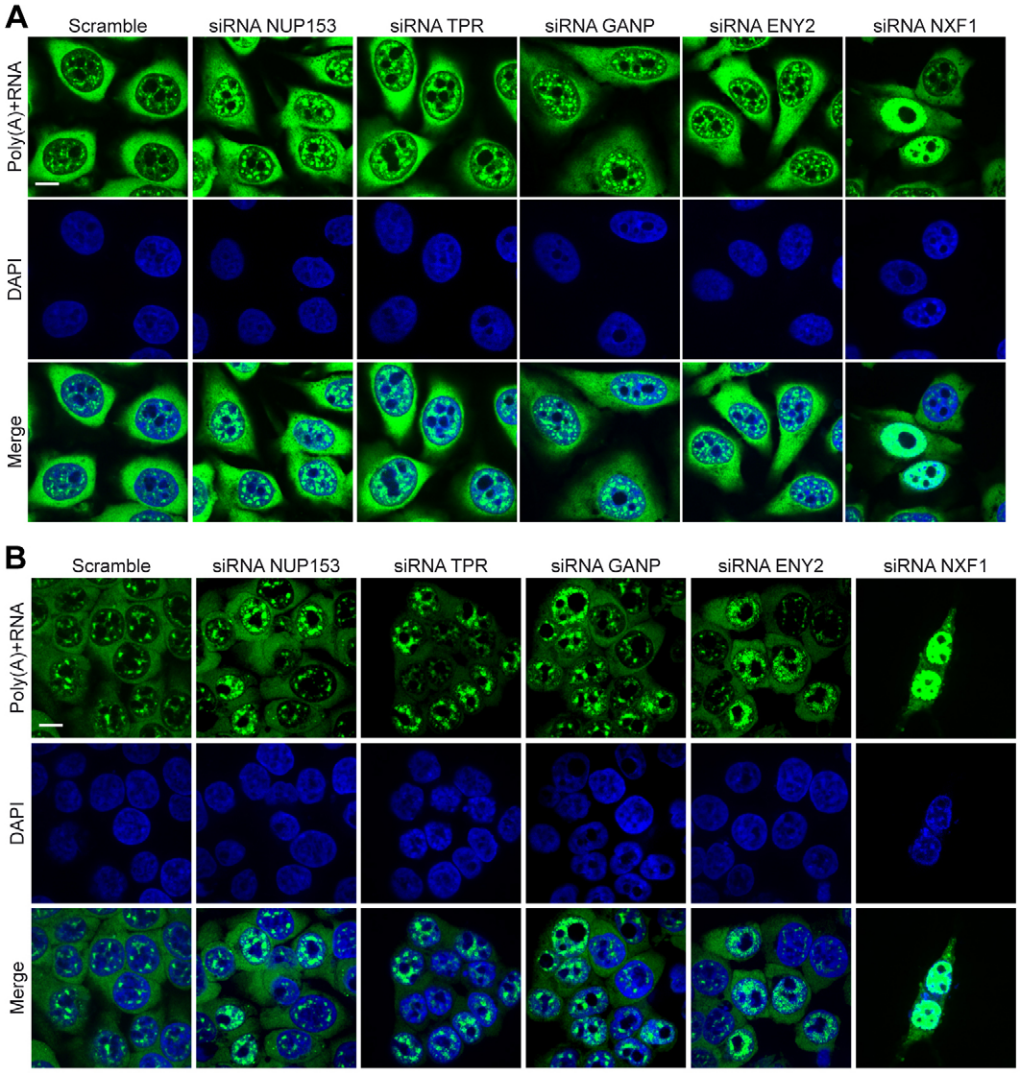

Fig. 7. Knockdown of TREX-2 subunits results in mRNA nuclear accumulation. (**A**,**B**) Hela (A) or HCT116 (B) cells were transfected with scramble siRNA or siRNAs targeting NUP153, TPR, GANP, ENY2 or NXF1 for 72 hours and the cellular distribution of poly(A)$^+$ mRNA was analyzed by FISH using an Alexa-Fluor-488-labelled poly(T) probe. Cells were analyzed by confocal microscopy. Scale bars: 10 μm.

Our live cell imaging experiments suggests tight interactions between TREX-2 subunits and baskets nucleoporins. In support of this, GANP, the scaffold protein of TREX-2, contains six FG repeats in its N-terminal region that could anchor the complex at the NPC. Intriguingly, proteomic characterization of the yeast NPC did not identify TREX-2 subunits as NPC-associated factors (Rout et al., 2000; Cronshaw et al., 2002). Similarly, our mass spectrometry and western blot analyses of ENY2-associated proteins did not reveal any associated nucleoporins. Nevertheless, a proteomic study in yeast has shown that Sac3, the yeast orthologue of GANP, can interact with several nucleoporins including Nup1, Mlp1 and Mlp2, the yeast homologues of NUP153 and TPR (Oeffinger et al., 2007). These seemingly contradictory results highlight that the biochemical demonstration of such nuclear membrane dependent interactions is extremely difficult and likely depends on subtle experimental variations. This is strengthening the need and importance of alternative approaches such as live cell imaging for the identification of NPC-associated factors.

Our FISH data show comparable nuclear accumulation of poly(A)$^+$ mRNA upon GANP, ENY2, NUP153 and TPR knockdown that is milder than that seen after NXF1 depletion. These data are in good agreement with previous studies showing that basket nucleoporins are not essential for mRNA export (Green et al., 2003) but are different from what has been previously published in *Drosophila* S2 or human HCT116 cells (Kurshakova et al., 2007; Wickramasinghe et al., 2010; Jani et al., 2012). Our experiments in HeLa and HCT116 cells reveal quantitative differences in poly(A)$^+$ mRNA nuclear accumulation after depletion of either basket nucleoporins or TREX-2 subunits suggesting functional differences between those cell types. Thus, we favor a model in which TREX-2 is an NPC basket-associated complex that helps the nucleo-cytoplasmic transport of export-competent mRNP particles. It remains to be determined whether the mRNA export phenotype is explained by a global function of TREX-2 on mRNA export or if a specific subset of mRNA is affected by its depletion.

Former studies in yeast reported that deletion of some but not all subunits of either TREX-2 or SAGA had an effect on gene re-localization at the nuclear periphery. Furthermore, a physical interaction between SAGA and TREX-2 has been proposed to be involved in gene gating (Cabal et al., 2006; Köhler et al., 2008). Such interaction was suggested to be mediated through Sus1 that is shared between the two complexes. However, the available

structural data do not support a direct interaction of the two complexes (Jani et al., 2009; Ellisdon et al., 2012; Jani et al., 2012). In addition, we show here that TREX-2 and the transcriptional co-activator SAGA do not interact with each other and are likely not functionally coupled in human cells. It is noteworthy that although gene gating has been reported in yeast and *Drosophila*, such a mechanism was never described in human cells. Moreover, our imaging experiments indicate that SAGA is exclusively nucleoplasmic and not enriched at the nuclear periphery. The SAGA-associated pool of ENY2 in the nucleoplasm did not exchange with the TREX-2-associated pool of ENY2 at the NPC basket. Together these observations do not support a colocalization of the two complexes at the nuclear periphery.

Overall, we propose that TREX-2 is a NPC-associated complex that has functional similarities with basket nucleoporins. These findings open new perspectives in the understanding of mRNA export mechanisms in metazoans. Finally, a number of studies indicate that the basket or associated proteins are involved in several nuclear functions beyond mRNA export, such as transcriptional regulation or chromatin organization (Strambio-De-Castillia et al., 2010). Further experiments are needed to elucidate whether TREX-2 is involved in such processes.

Materials and Methods

Immunoprecipitation

For immunoprecipitation cells were resuspended volume to volume in 10 mM Tris-HCl pH 8.0, 1.5 mM $MgCl_2$, 10 mM KCl, protease inhibitors (from Roche) and dounced 20 times using a B dounce homogenizer. After centrifugation, nuclei were resuspended volume to volume in 20 mM Tris-HCl pH 8.0, 25% glycerol, 1.5 mM $MgCl_2$, 450 mM NaCl, 1 mM $CaCl_2$, protease inhibitors (from Roche) and incubated 30 minutes on ice with occasional mixing. After 10 minutes centrifugation at 10,000 rpm soluble nuclear extracts were transferred in a new tube. For ENY2-FLAG-HA and FLAG-HA-SPT3 sequential immunoprecipitation, nuclear extracts were incubated overnight at 4℃ with anti-FLAG M2 Sepharose beads (Sigma-Aldrich), washed three times in IP500 buffer [25 mM Tris-HCl pH 8.0; 5 mM $MgCl_2$; 10% glycerol; 0.1% NP40; 0.3 mM DTT; 500 mM KCl; Protease Inhibitor (Roche)], three times in IP100 buffer (25 mM Tris-HCl pH 8.0; 5 mM $MgCl_2$; 10% glycerol; 0.1% NP40; 0.3 mM DTT; 100 mM KCl; Roche Protease Inhibitor) buffer. After elution with a FLAG specific peptide, eluted material was incubated overnight at 4℃ with anti-HA sepharose beads (Invitrogen), washed three times in IP500 buffer, three times in IP100 buffer. Elution was performed using an HA specific peptide. EGFP fusions proteins were immunoprecipitated as above with anti-HA sepharose beads (Invitrogen). RNase A treated (200 µg/ml) nuclear extracts were prepared in 20 mM Tris-HCl pH 8.0, 25% Glycerol, 1.5 mM $MgCl_2$, 150 mM NaCl, 1 mM $CaCl_2$, 0.1% IGEPAL CA-630 (Sigma) protease inhibitors (from Roche). Immunoprecipitation and washes were done in 150 mM KCl.

Nanoflow LC-MS/MS and MudPIT mass spectrometry analyses

Immunoprecipitated material was analysed by nanoflow LC-MS/MS on an LTQ-Orbitrap thermo mass spectrometer at the proteomics center of the Erasmus University Medical Center in Rotterdam (as described in Krebs et al., 2010). For MudPIT analyses (Paoletti et al., 2006), samples were processed by the proteomics platform of the IGBMC.

Antibodies

Antibodies against GANP (ab113295), RNA polymerase II (ab5131), NXF1 (ab50609), TPR (ab84516), NUP358/RANBP2 (ab24276), Lamin A/C (ab8984), EGFP (ab290) and the nuclear pore complex (ab24609) were from Abcam. Antibodies against the FLAG epitope (F7425), anti-5FU antibody (B2531) and Tubulin (T6557) were from Sigma-Aldrich. Antibody against the HA epitope was from Roche. Antibody to CETN2 (sc27793) was from Santa Cruz. The CETN3 antibody used for immunofluorescence was a kind gift from Dr Uwe Wolfrum. TREX-2 specific rabbit polyclonal antibodies were raised against the following peptides where (C) indicates an added cysteine that was used for coupling the peptide to activated ovalbumine: GANP serum 2988 and 2987: (C)SSLLNKSSPVKKPSL; PCID2 serum 2990: ITINQYLQQVYE(C); CETN3 serum 2985:(C)EINQEEFIAIMTGDI. All sera but 2990 were purified using Sulfolink Coupling Gel (Pierce) according to the manufacturer's instructions. All the other antibodies used in this study were described elsewhere: TRRAP 2TRR-2D5 (Helmlinger et al., 2004); GCN5 2GC-2C11 (Brand et al., 2001); ATXN7L3 2325 and 2ATX-2B1(Zhao et al., 2008); ADA3 2678 (Nagy et al., 2009); TAF12 22TA-2A1 (Mengus et al., 1995); SGF29 2461 (Nagy et al., 2009). For immunofluorescence all secondary antibodies used in this study were Alexa Fluor Antibodies from Invitrogen. Western blots were revealed using peroxydase conjuguated secondary antibodies from Jackson Immunoresearch Laboratories.

Cell culture and treatments

HeLa S3 cells expressing the FLAG-HA tagged version of ENY2 and SPT3 were grown at 37℃ in Dulbecco's modified Eagle's medium (Invitrogen) supplemented with 4 g/l glucose, 10% FCS and gentamycin. HeLa cells used for immunofluorescence were grown at 37℃ in Dulbecco's modified Eagle's medium (Invitrogen) supplemented with 1 g/l glucose, 10% fetal calf serum and gentamycin. For proteasome inhibition experiments cells were incubated for 15 hours with medium containing 20 µM MG132 (calbiochem). For transcription inhibition experiments cells were incubated 4–6 hours with 5 µg/ml actinomycin D (Sigma-Aldrich) or 50 µg/ml α-amanitin (Sigma-Aldrich). To evaluate for transcription inhibition cells were further incubated with 1 mM 5-fluorouridine (Sigma-Aldrich) for 15–20 minutes. Incorporation of the modified nucleotide was assessed by staining the cells with an anti 5-FU antibody from Sigma-Aldrich.

Immunofluorescence

For indirect immunofluorescence cells were grown on glass coverslips and fixed with 2% formaldehyde in 1X PBS for 10 minutes, washed three times 5 minutes in 1× PBS and permeabilized for 10 minutes in 0.1% Triton X-100 in 1× PBS. Cells were then blocked 30 minutes in blocking buffer containing 1× PBS and 10% goat serum and incubated for 1 hour at 37℃ with the primary antibodies diluted in blocking buffer. Cells were then washed three times in 1× PBS containing 0.1% Triton X-100 and incubated with the secondary antibody conjugated to Alexa Fluor 488 or Alexa Fluor 594 (Invitrogen) in blocking buffer for 1 hour at 37℃. Cells were then washed three times in 1× PBS containing 0.1% Triton X-100 and mounted on Vectashield (Vector Laboratories). For the anti PCID2 (2990) antibody cells were alternatively fixed in 4% formaldehyde and permeabilized with 1× PBS containing 0.5% Triton X-100. In the Digitonin permeabilization experiment, cells were first fixed with 2% formaldehyde in 1× PBS for 10 minutes and further permeabilized with 0.004% of Digitonin (Sigma-Aldrich). Images were analyzed using the imageJ software (NIH). For fluorescence distribution analysis, a line width of 20 pixels was used.

siRNA transfection

Scramble (AM4635), anti-PCID2 (ID:s31530, ID:s31531, ID:s31532) and anti-ENY2 (ID:s32449, ID:s32447, ID:s226899) siRNA were purchased from Ambion Anti-GANP siRNA were described elsewhere (Wickramasinghe et al., 2010). Additionally, anti-NUP153 siRNA (Cat No.: D-005283-01) as well as ON-TARGET plus SMART pool anti-ENY2 (CatNO.: L-018808-01), anti-TPR (Cat No.: L-010548-00), anti-NXF1 (Cat No.: L-013680-01) and anti-CETN3 (CatNO.: L-011832-00) siRNA were purchased from Dharmacon. All siRNA were transfected in HeLa cells using Lipofectamine®2000 according to the manufacturer's instructions.

Poly(A)+ RNA FISH

Cells were grown on glass coverslips for 24 hours and then transfected for 72 hours with siRNA prior to performing poly(A)+ RNA FISH. Cells were fixed in 4% formaldehyde in 1× PBS for 10 minutes, washed in 1× PBS and permeabilized 5 minutes on ice with 0.5% Triton X-100 in 1× PBS. Cells were incubated 5 minutes in 1× PBS followed by 5 minutes in 2× SSC (0.3 M NaCl; 0,03 M sodium citrate) and prehybridized for 1 hour in hybridization buffer (50% formamide, 2× SSC, 1 mg/ml BSA, 1 mg/ml tRNA, 10% dextran sulfate). The cells were hybridized overnight in hybridization buffer containing 100 pg/µl Alexa-Fluor-488-oligo$(dT)_{50}$, washed three times in 2× SSC, three times in 1× SSC, three times in 0.5× SSC (all washes at 37℃ for 5 minutes each) followed by a final wash of 5 minutes in 1× PBS before mounting the cells using Vectashield (Vector Laboratories).

Establishment of stable cell line

Human cDNA clones of ENY2 and SPT3 were amplified by PCR with primers incorporating *Xho*I/*Not*I recognition sites and subcloned into the *Xho*I/*Not*I sites of the pREV-HTF retroviral vector containing a C-terminal (ENY2) or N-terminal (SPT3) FLAG-HA peptide sequence. Stable cell lines were then generated by retroviral infection as described in (Nakatani and Ogryzko, 2003). HeLa EGFP-ENY2 and EGFP-PCID2 stable cell lines were generated in two steps. First, the cDNA of the EGFP protein was PCR amplified with primers incorporating a 5′*Hin*dIII restriction site followed by the HA peptide sequence and a 3′ linker sequence followed by a *Xho*I site. PCR products were cloned into the *Hin*dIII/*Xho*I site of the pcDNA3.1+ vector (Invitrogen). As a second step, the full length cDNA of ENY2 or PCID2 was amplified by PCR with primers incorporating *Xho*I/*Xba*I recognition sites and subcloned into the *Xho*I/*Xba*I sites of the pcDNA3.1+ vector.

HeLa cells were transfected using Lipofectamine 2000® according to the manufacturer's instructions. Twenty-four hours after transfection cells were diluted to allow individual clone selection in medium containing G418 (500 μg/ml). After 2 weeks of G418 selection, individual clones were isolated and further subcloned. All experiments presented were made with monoclonal EGFP-ENY2 and EGFP-PCID2 cell lines.

Microscopy

For immunofluorescence, cells were analyzed using a DMI 6000 Leica microscope using a HCX Pl Apo 63× 1.4 lens, a CSU22 Yokogawa confocal spinning disk and an ANDOR iXon 897+ EMCCD camera. For live cell imaging experiments cells were grown on Lab-Tek™ Chamber Slide™ System (Nunc). The optical set-up used for FRAP and FLIP measurements and video imaging was based on a Nikon TE2000-E inverted microscope equipped with a CSU22 Yokogawa confocal spinning disk and a 60× Plan Apo NA 1.4 lens. Excitation used a Melles-Griot 100 mW argon-krypton laser. Emission was filtered using Chroma filter set (BP 525/50 nm). Photonic Instrument MicroPoint laser technology (491 nm, 50 mW) was used to create a bleached spot in the sample (50 milliseconds laser bleach duration per point). For FRAP experiments EGFP-ENY2 and EGFP-PCID2 images were denoised using algorithm described in (Boulanger et al., 2010). For the experiments shown in supplementary material Fig. S7, fluorescence has been acquired with an INCell1000 Analyzer workstation (GE LifeSciences) using a 10× magnification objective. We analyzed the pictures with the Multi Target Analysis software (GE LifeScience) by segmenting the nucleus of the cells according to the DAPI staining. The nuclear Poly(A)$^+$ mRNA foci have been detected in the nucleus to study their number and area in the different silencing conditions using the Multi Target Analysis software (GE LifeScience).

Acknowledgements

We are grateful to M.E. Torres-Padilla and Y. Shav-Tal for critical reading of the manuscript; A. Hamiche for the pREV plasmid; C.L. Tomasetto for the pEYFP-C1-NXF1 and pEGFP-C1-NUP153 plasmids; P. Eberling for peptide synthesis; G. Duval for generating antibodies, and the cell culture facility of the IGBMC. We are grateful to U. Wolfrum for the CETN3 antibody, J. Demmers for proteomic analysis, M. Koch and P. Kessler for help in the microscopy experiments and the PICT-IBISA microscopy platform of the Curie Institute for help in FRAP and FLIP experiments. The authors declare that they have no conflict of interest.

Author contribution

D.U. designed, performed, analyzed all experiments and wrote the manuscript. J.B. and M.S. established and performed the initial characterization of the HeLa ENY2-FLAG-HA and FLAG-HA-SPT3 cell lines. F.W. performed and analyzed FRAP and FLIP experiments with D.U. M.F. performed and analyzed the MudPIT experiments. B.F. and L.B. performed the high throughput analysis of data obtained in Fig. 7. D.D. and L.T. designed experiments, analyzed the data and wrote the manuscript.

Funding

J.B. was a recipient of a fellowship from the Fondation Pour la Recherche Médicale. This work was funded by grants from ANR (ANR-09-MNPS-023; ANR-10-INTB-1201; ANR-09-BLAN-0266), the EU (SAGATAC, EUTRACC, LSHG-CT-2007-037445 and EPIDIACAN), INCA (2008 UBican) and CNRS (LEA-SkinChroma).

Supplementary material available online at
http://jcs.biologists.org/lookup/suppl/doi:10.1242/jcs.118000/-/DC1

References

Abruzzi, K. C., Lacadie, S. and Rosbash, M. (2004). Biochemical analysis of TREX complex recruitment to intronless and intron-containing yeast genes. *EMBO J.* **23**, 2620-2631.

Antonin, W., Ellenberg, J. and Dultz, E. (2008). Nuclear pore complex assembly through the cell cycle: regulation and membrane organization. *FEBS Lett.* **582**, 2004-2016.

Bodoor, K., Shaikh, S., Salina, D., Raharjo, W. H., Bastos, R., Lohka, M. and Burke, B. (1999). Sequential recruitment of NPC proteins to the nuclear periphery at the end of mitosis. *J. Cell Sci.* **112**, 2253-2264.

Boulanger, J., Kervrann, C., Bouthemy, P., Elbau, P., Sibarita, J. B. and Salamero, J. (2010). Patch-based nonlocal functional for denoising fluorescence microscopy image sequences. *IEEE Trans. Med. Imaging* **29**, 442-454.

Brand, M., Moggs, J. G., Oulad-Abdelghani, M., Lejeune, F., Dilworth, F. J., Stevenin, J., Almouzni, G. and Tora, L. (2001). UV-damaged DNA-binding protein in the TFTC complex links DNA damage recognition to nucleosome acetylation. *EMBO J.* **20**, 3187-3196.

Burke, B. and Ellenberg, J. (2002). Remodelling the walls of the nucleus. *Nat. Rev. Mol. Cell Biol.* **3**, 487-497.

Cabal, G. G., Genovesio, A., Rodríguez-Navarro, S., Zimmer, C., Gadal, O., Lesne, A., Buc, H., Feuerbach-Fournier, F., Olivo-Marin, J. C., Hurt, E. C. et al. (2006). SAGA interacting factors confine sub-diffusion of transcribed genes to the nuclear envelope. *Nature* **441**, 770-773.

Cronshaw, J. M., Krutchinsky, A. N., Zhang, W., Chait, B. T. and Matunis, M. J. (2002). Proteomic analysis of the mammalian nuclear pore complex. *J. Cell Biol.* **158**, 915-927.

Dimitrova, D. S. (2006). Nuclear transcription is essential for specification of mammalian replication origins. *Genes Cells* **11**, 829-844.

Dultz, E., Zanin, E., Wurzenberger, C., Braun, M., Rabut, G., Sironi, L. and Ellenberg, J. (2008). Systematic kinetic analysis of mitotic dis- and reassembly of the nuclear pore in living cells. *J. Cell Biol.* **180**, 857-865.

Ellisdon, A. M., Jani, D., Köhler, A., Hurt, E. and Stewart, M. (2010). Structural basis for the interaction between yeast Spt-Ada-Gcn5 acetyltransferase (SAGA) complex components Sgf11 and Sus1. *J. Biol. Chem.* **285**, 3850-3856.

Ellisdon, A. M., Dimitrova, L., Hurt, E. and Stewart, M. (2012). Structural basis for the assembly and nucleic acid binding of the TREX-2 transcription-export complex. *Nat. Struct. Mol. Biol.* **19**, 328-336.

Faza, M. B., Kemmler, S., Jimeno, S., González-Aguilera, C., Aguilera, A., Hurt, E. and Panse, V. G. (2009). Sem1 is a functional component of the nuclear pore complex-associated messenger RNA export machinery. *J. Cell Biol.* **184**, 833-846.

Fischer, T., Strässer, K., Rácz, A., Rodríguez-Navarro, S., Oppizzi, M., Ihrig, P., Lechner, J. and Hurt, E. (2002). The mRNA export machinery requires the novel Sac3p-Thp1p complex to dock at the nucleoplasmic entrance of the nuclear pores. *EMBO J.* **21**, 5843-5852.

Fischer, T., Rodríguez-Navarro, S., Pereira, G., Rácz, A., Schiebel, E. and Hurt, E. (2004). Yeast centrin Cdc31 is linked to the nuclear mRNA export machinery. *Nat. Cell Biol.* **6**, 840-848.

Frosst, P., Guan, T., Subauste, C., Hahn, K. and Gerace, L. (2002). Tpr is localized within the nuclear basket of the pore complex and has a role in nuclear protein export. *J. Cell Biol.* **156**, 617-630.

Giessl, A., Pulvermüller, A., Trojan, P., Park, J. H., Choe, H. W., Ernst, O. P., Hofmann, K. P. and Wolfrum, U. (2004). Differential expression and interaction with the visual G-protein transducin of centrin isoforms in mammalian photoreceptor cells. *J. Biol. Chem.* **279**, 51472-51481.

Green, D. M., Johnson, C. P., Hagan, H. and Corbett, A. H. (2003). The C-terminal domain of myosin-like protein 1 (Mlp1p) is a docking site for heterogeneous nuclear ribonucleoproteins that are required for mRNA export. *Proc. Natl. Acad. Sci. USA* **100**, 1010-1015.

Grüter, P., Tabernero, C., von Kobbe, C., Schmitt, C., Saavedra, C., Bachi, A., Wilm, M., Felber, B. K. and Izaurralde, E. (1998). TAP, the human homolog of Mex67p, mediates CTE-dependent RNA export from the nucleus. *Mol. Cell* **1**, 649-659.

Helmlinger, D., Hardy, S., Sasorith, S., Klein, F., Robert, F., Weber, C., Miguet, L., Potier, N., Van-Dorsselaer, A., Wurtz, J. M. et al. (2004). Ataxin-7 is a subunit of GCN5 histone acetyltransferase-containing complexes. *Hum. Mol. Genet.* **13**, 1257-1265.

Huertas, P. and Aguilera, A. (2003). Cotranscriptionally formed DNA:RNA hybrids mediate transcription elongation impairment and transcription-associated recombination. *Mol. Cell* **12**, 711-721.

Jani, D., Lutz, S., Marshall, N. J., Fischer, T., Köhler, A., Ellisdon, A. M., Hurt, E. and Stewart, M. (2009). Sus1, Cdc31, and the Sac3 CID region form a conserved interaction platform that promotes nuclear pore association and mRNA export. *Mol. Cell* **33**, 727-737.

Jani, D., Lutz, S., Hurt, E., Laskey, R. A., Stewart, M. and Wickramasinghe, V. O. (2012). Functional and structural characterization of the mammalian TREX-2 complex that links transcription with nuclear messenger RNA export. *Nucleic Acids Res.* **40**, 4562-4573.

Jimeno, S., Rondón, A. G., Luna, R. and Aguilera, A. (2002). The yeast THO complex and mRNA export factors link RNA metabolism with transcription and genome instability. *EMBO J.* **21**, 3526-3535.

Köhler, A., Pascual-García, P., Llopis, A., Zapater, M., Posas, F., Hurt, E. and Rodríguez-Navarro, S. (2006). The mRNA export factor Sus1 is involved in Spt/Ada/Gcn5 acetyltransferase-mediated H2B deubiquitinylation through its interaction with Ubp8 and Sgf11. *Mol. Biol. Cell* **17**, 4228-4236.

Köhler, A., Schneider, M., Cabal, G. G., Nehrbass, U. and Hurt, E. (2008). Yeast Ataxin-7 links histone deubiquitination with gene gating and mRNA export. *Nat. Cell Biol.* **10**, 707-715.

Köhler, A., Zimmerman, E., Schneider, M., Hurt, E. and Zheng, N. (2010). Structural basis for assembly and activation of the heterotetrameric SAGA histone H2B deubiquitinase module. *Cell* **141**, 606-617.

Krebs, A. R., Demmers, J., Karmodiya, K., Chang, N. C., Chang, A. C. and Tora, L. (2010). ATAC and Mediator coactivators form a stable complex and regulate a set of non-coding RNA genes. *EMBO Rep.* **11**, 541-547.

Kurshakova, M. M., Krasnov, A. N., Kopytova, D. V., Shidlovskii, Y. V., Nikolenko, J. V., Nabirochkina, E. N., Spehner, D., Schultz, P., Tora, L. and Georgieva, S. G. (2007). SAGA and a novel Drosophila export complex anchor efficient transcription and mRNA export to NPC. *EMBO J.* **26**, 4956-4965.

Lang, G., Bonnet, J., Umlauf, D., Karmodiya, K., Koffler, J., Stierle, M., Devys, D. and Tora, L. (2011). The tightly controlled deubiquitination activity of the human SAGA complex differentially modifies distinct gene regulatory elements. *Mol. Cell. Biol.* **31**, 3734-3744.

Lu, Q., Tang, X., Tian, G., Wang, F., Liu, K., Nguyen, V., Kohalmi, S. E., Keller, W. A., Tsang, E. W., Harada, J. J. et al. (2010). Arabidopsis homolog of the yeast TREX-2 mRNA export complex: components and anchoring nucleoporin. *Plant J.* **61**, 259-270.

Masuda, S., Das, R., Cheng, H., Hurt, E., Dorman, N. and Reed, R. (2005). Recruitment of the human TREX complex to mRNA during splicing. *Genes Dev.* **19**, 1512-1517.

Mengus, G., May, M., Jacq, X., Staub, A., Tora, L., Chambon, P. and Davidson, I. (1995). Cloning and characterization of hTAFII18, hTAFII20 and hTAFII28: three subunits of the human transcription factor TFIID. *EMBO J.* **14**, 1520-1531.

Middendorp, S., Paoletti, A., Schiebel, E. and Bornens, M. (1997). Identification of a new mammalian centrin gene, more closely related to Saccharomyces cerevisiae CDC31 gene. *Proc. Natl. Acad. Sci. USA* **94**, 9141-9146.

Moore, M. J. and Proudfoot, N. J. (2009). Pre-mRNA processing reaches back to transcription and ahead to translation. *Cell* **136**, 688-700.

Nagy, Z., Riss, A., Romier, C., le Guezennec, X., Dongre, A. R., Orpinell, M., Han, J., Stunnenberg, H. and Tora, L. (2009). The human SPT20-containing SAGA complex plays a direct role in the regulation of endoplasmic reticulum stress-induced genes. *Mol. Cell. Biol.* **29**, 1649-1660.

Nakatani, Y. and Ogryzko, V. (2003). Immunoaffinity purification of mammalian protein complexes. *Methods Enzymol.* **370**, 430-444.

Oeffinger, M., Wei, K. E., Rogers, R., DeGrasse, J. A., Chait, B. T., Aitchison, J. D. and Rout, M. P. (2007). Comprehensive analysis of diverse ribonucleoprotein complexes. *Nat. Methods* **4**, 951-956.

Paoletti, A. C., Parmely, T. J., Tomomori-Sato, C., Sato, S., Zhu, D., Conaway, R. C., Conaway, J. W., Florens, L. and Washburn, M. P. (2006). Quantitative proteomic analysis of distinct mammalian Mediator complexes using normalized spectral abundance factors. *Proc. Natl. Acad. Sci. USA* **103**, 18928-18933.

Piruat, J. I. and Aguilera, A. (1998). A novel yeast gene, THO2, is involved in RNA pol II transcription and provides new evidence for transcriptional elongation-associated recombination. *EMBO J.* **17**, 4859-4872.

Rabut, G., Doye, V. and Ellenberg, J. (2004). Mapping the dynamic organization of the nuclear pore complex inside single living cells. *Nat. Cell Biol.* **6**, 1114-1121.

Resendes, K. K., Rasala, B. A. and Forbes, D. J. (2008). Centrin 2 localizes to the vertebrate nuclear pore and plays a role in mRNA and protein export. *Mol. Cell. Biol.* **28**, 1755-1769.

Rodríguez-Navarro, S., Fischer, T., Luo, M. J., Antúnez, O., Brettschneider, S., Lechner, J., Pérez-Ortín, J. E., Reed, R. and Hurt, E. (2004). Sus1, a functional component of the SAGA histone acetylase complex and the nuclear pore-associated mRNA export machinery. *Cell* **116**, 75-86.

Rout, M. P., Aitchison, J. D., Suprapto, A., Hjertaas, K., Zhao, Y. and Chait, B. T. (2000). The yeast nuclear pore complex: composition, architecture, and transport mechanism. *J. Cell Biol.* **148**, 635-652.

Samara, N. L., Datta, A. B., Berndsen, C. E., Zhang, X., Yao, T., Cohen, R. E. and Wolberger, C. (2010). Structural insights into the assembly and function of the SAGA deubiquitinating module. *Science* **328**, 1025-1029.

Segref, A., Sharma, K., Doye, V., Hellwig, A., Huber, J., Lührmann, R. and Hurt, E. (1997). Mex67p, a novel factor for nuclear mRNA export, binds to both poly(A)+ RNA and nuclear pores. *EMBO J.* **16**, 3256-3271.

Strambio-De-Castillia, C., Niepel, M. and Rout, M. P. (2010). The nuclear pore complex: bridging nuclear transport and gene regulation. *Nat. Rev. Mol. Cell Biol.* **11**, 490-501.

Strässer, K. and Hurt, E. (2000). Yra1p, a conserved nuclear RNA-binding protein, interacts directly with Mex67p and is required for mRNA export. *EMBO J.* **19**, 410-420.

Stutz, F., Bachi, A., Doerks, T., Braun, I. C., Séraphin, B., Wilm, M., Bork, P. and Izaurralde, E. (2000). REF, an evolutionary conserved family of hnRNP-like proteins, interacts with TAP/Mex67p and participates in mRNA nuclear export. *RNA* **6**, 638-650.

Sukegawa, J. and Blobel, G. (1993). A nuclear pore complex protein that contains zinc finger motifs, binds DNA, and faces the nucleoplasm. *Cell* **72**, 29-38.

Trojan, P., Krauss, N., Choe, H. W., Giessl, A., Pulvermüller, A. and Wolfrum, U. (2008). Centrins in retinal photoreceptor cells: regulators in the connecting cilium. *Prog. Retin. Eye Res.* **27**, 237-259.

Wickramasinghe, V. O., McMurtrie, P. I., Mills, A. D., Takei, Y., Penrhyn-Lowe, S., Amagase, Y., Main, S., Marr, J., Stewart, M. and Laskey, R. A. (2010). mRNA export from mammalian cell nuclei is dependent on GANP. *Curr. Biol.* **20**, 25-31.

Wilmes, G. M., Bergkessel, M., Bandyopadhyay, S., Shales, M., Braberg, H., Cagney, G., Collins, S. R., Whitworth, G. B., Kress, T. L., Weissman, J. S. et al. (2008). A genetic interaction map of RNA-processing factors reveals links between Sem1/Dss1-containing complexes and mRNA export and splicing. *Mol. Cell* **32**, 735-746.

Yao, W., Roser, D., Köhler, A., Bradatsch, B., Bassler, J. and Hurt, E. (2007). Nuclear export of ribosomal 60S subunits by the general mRNA export receptor Mex67-Mtr2. *Mol. Cell* **26**, 51-62.

Yao, W., Lutzmann, M. and Hurt, E. (2008). A versatile interaction platform on the Mex67-Mtr2 receptor creates an overlap between mRNA and ribosome export. *EMBO J.* **27**, 6-16.

Zenklusen, D., Vinciguerra, P., Wyss, J. C. and Stutz, F. (2002). Stable mRNP formation and export require cotranscriptional recruitment of the mRNA export factors Yra1p and Sub2p by Hpr1p. *Mol. Cell. Biol.* **22**, 8241-8253.

Zhao, Y., Lang, G., Ito, S., Bonnet, J., Metzger, E., Sawatsubashi, S., Suzuki, E., Le Guezennec, X., Stunnenberg, H. G., Krasnov, A. et al. (2008). A TFTC/STAGA module mediates histone H2A and H2B deubiquitination, coactivates nuclear receptors, and counteracts heterochromatin silencing. *Mol. Cell* **29**, 92-101.